Coupling of MSC/NASTRAN and BEM Structural Matrices

M. J. McNamee, K. L. Leung and P. B. Zavareh

United Technologies Corporation, USBI Co.,
Huntsville, Alabama 35807, U.S.A.

Abstract

Accurate stress analysis using a combination of the Finite Element Method (FEM) and the Boundary Element Method (BEM) is achieved by coupling MSC/NASTRAN with symmetric BEM structural matrices through the use of the external superelement technique. A DMAP procedure is developed to incorporate the symmetric stiffness matrix derived by the BEM into the global stiffness matrix generated by MSC/NASTRAN. This coupled MSC/NASTRAN-BEM analysis procedure provides a way to exploit the versatility of MSC/NASTRAN in handling wide classes of engineering problems, including those involving nonlinearity and inhomogeneity, while maintaining the accuracy of the BEM in areas of crack and stress concentration. Several analysis examples are given to illustrate the usefulness of the proposed technique.

Introduction

The major strength of the finite element method (FEM), such as in MSC/NASTRAN, is its versatility in handling various classes of engineering problems involving nonlinearity and inhomogeneity. The boundary element method (BEM) has strengths in handling problems with stress concentrations and infinite domains. A desirable situation for the engineer is a coupling of FEM and BEM methods to capitalize on the strengths of each method. Coupling of the two methods allows effective solution of problems of a localized nature directly within the global model. Two typical examples of such coupling are as follows:

(a) Local stress concentration in a complex structure (Figure 1)

In this case the BEM can be employed in the vicinity of a high stress gradient, whereas the FEM can easily model the rest of the complex structure which may involve inhomogeneity, anisotropy or nonlinearity.

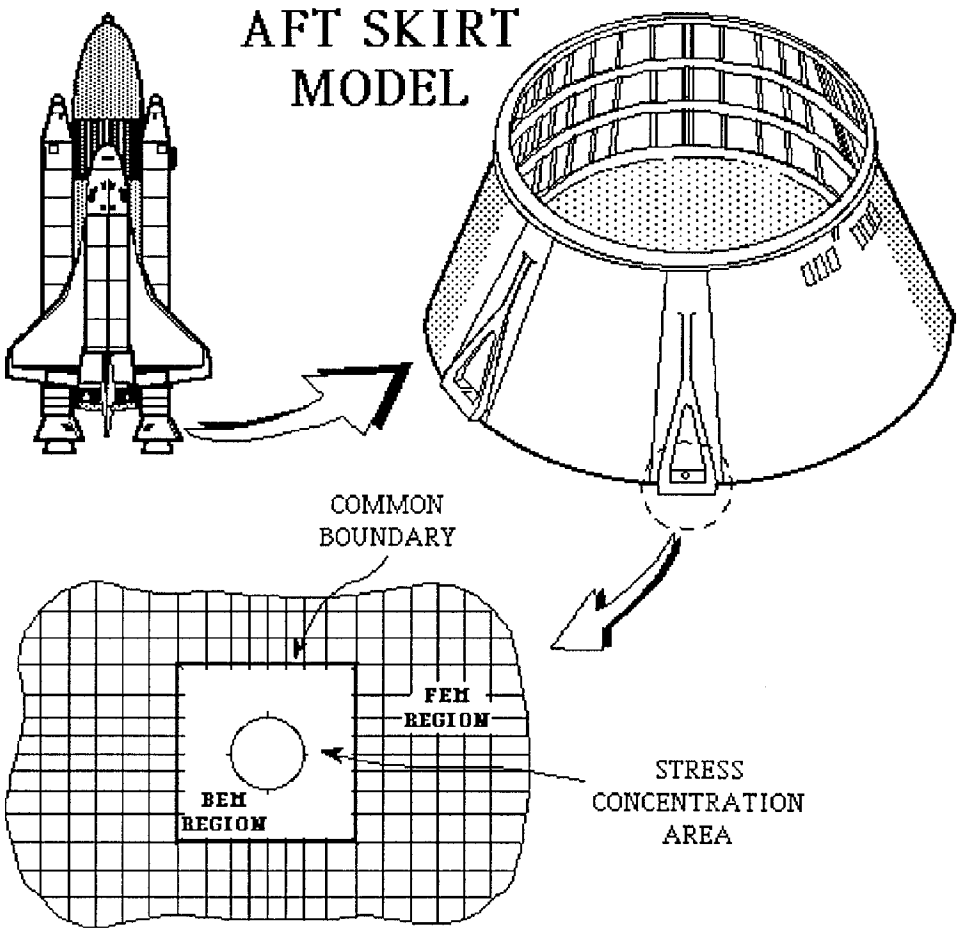

Figure 1. Local Stress Concentration Around a Bolt Hole

(b) Local nonlinearity or inhomogeneity in the infinite domain (Figure 2)

In this case the FEM can be used to handle the local nonlinearity or inhomogeneity, whereas the BEM can be used to model the infinite or semi-infinite domain which is assumed to be linear and homogeneous.

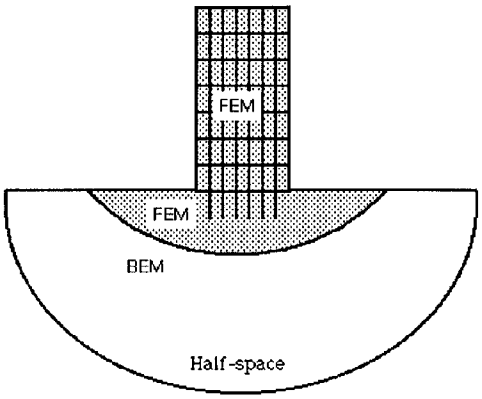

Figure 2. Local Inhomogeneity on the Semi-infinite Half-space

One of the major difficulties of BEM/FEM coupling is the nonsymetrical and fully populated nature of the stiffness matrix derived from a conventional BEM formulation. In order to cope with this problem, Zienkiewicz et. al. [1] and Brebbia and Georgiou [2] forced a symmetrization of the conventional BEM stiffness matrix on the basis of energy or error minimization considerations. This forced symmetrization technique has been followed by Kohno et. al. [3] who reported a hybrid method of BEM and FEM analysis by means of the external superelement function of MSC/NASTRAN. However, as pointed out by Tullberg and Bolteus [4] and Mang et. al. [5], this symmetrization technique results in a loss of equilibrium in a region near the interface. In the present work at United Technologies/USBI Co. a hybrid displacement variational formulation for the BEM is employed to produce symmetrical stiffness matrices [6] that can be introduced into MSC/NASTRAN. This paper will focus on the method used to introduce symmetric BEM matrices into MSC/NASTRAN and the results of several example problems.

Problem Definition

Coupling the BEM matrices to the FEM matrices of MSC/NASTRAN requires solving two problems. The first problem is casting the BEM matrix in a form that is compatible with the MSC/NASTRAN FEM formulation. The present work done at United Technologies/USBI Co. uses a hybrid displacement variational formulation for elastostatics problems. This formulation provides a symmetrical BEM stiffness matrix that involves nodal displacement and nodal forces on the boundary, allowing a consistent coupling with MSC/NASTRAN by enforcing nodal equilibrium and compatibility at the BEM - MSC/NASTRAN interface. The details of this formulation can be found in references [6-8].

The second problem, and main subject of this paper, is the method of introducing and merging the BEM matrix into the MSC/NASTRAN solution. The matrix merging method should require the least amount of effort by the end user while maintaining accuracy and minimizing procedure errors. MSC/NASTRAN provides a variety of methods for importing and merging an external matrix into one of the standard subDMAP solutions [9,10]. The bulk data cards GENEL, DMI and DMIG provide three methods of introducing an external matrix into MSC/NASTRAN. Use of these bulk data cards requires more than a casual knowledge of MSC/NASTRAN matrix definition. After the matrix is imported by the bulk data cards, it must be correctly combined with the correct MSC/NASTRAN matrix. Thus some DMAP programming is required. The use of bulk data cards can be eliminated by using the INPUTT2 or INPUTT4 DMAP modules. These two modules still require a fair amount of DMAP programming and knowledge of matrix definitions. All of these methods required too much effort by the end user. A method with higher automation and avoiding any DMAP programming was sought.

The experience with superelements both internal and external provided the baseline for developing a method to introduce BEM matrices into MSC/NASTRAN. The external superelement method was chosen to minimize DMAP programming and use the preprogrammed DMAP logic of superelements to merge the BEM and FEM matrices. Interface consistency rules for external superelements are not waived by this method. The method simply replaces dummy external superelement matrices with the BEM matrices. The steps used to import a BEM matrix into the MSC/NASTRAN database through an external superelement is shown in Figure 3.

The BEM code is set up to reduce the BEM matrix to the interface degrees of freedom and write the reduced BEM matrix to an ASCII file in the grid point order specified on the CSUPER connection card. External superelement interface rules were applied to build a standard translator program. The translator program reads the BEM matrix file and then writes a file in a format compatible with the INPUTT4 DMAP module. The standard translator eliminates writing or modifying a translator for each analysis by the end user. Further automation can be accomplished by embedding the translator into the BEM code.

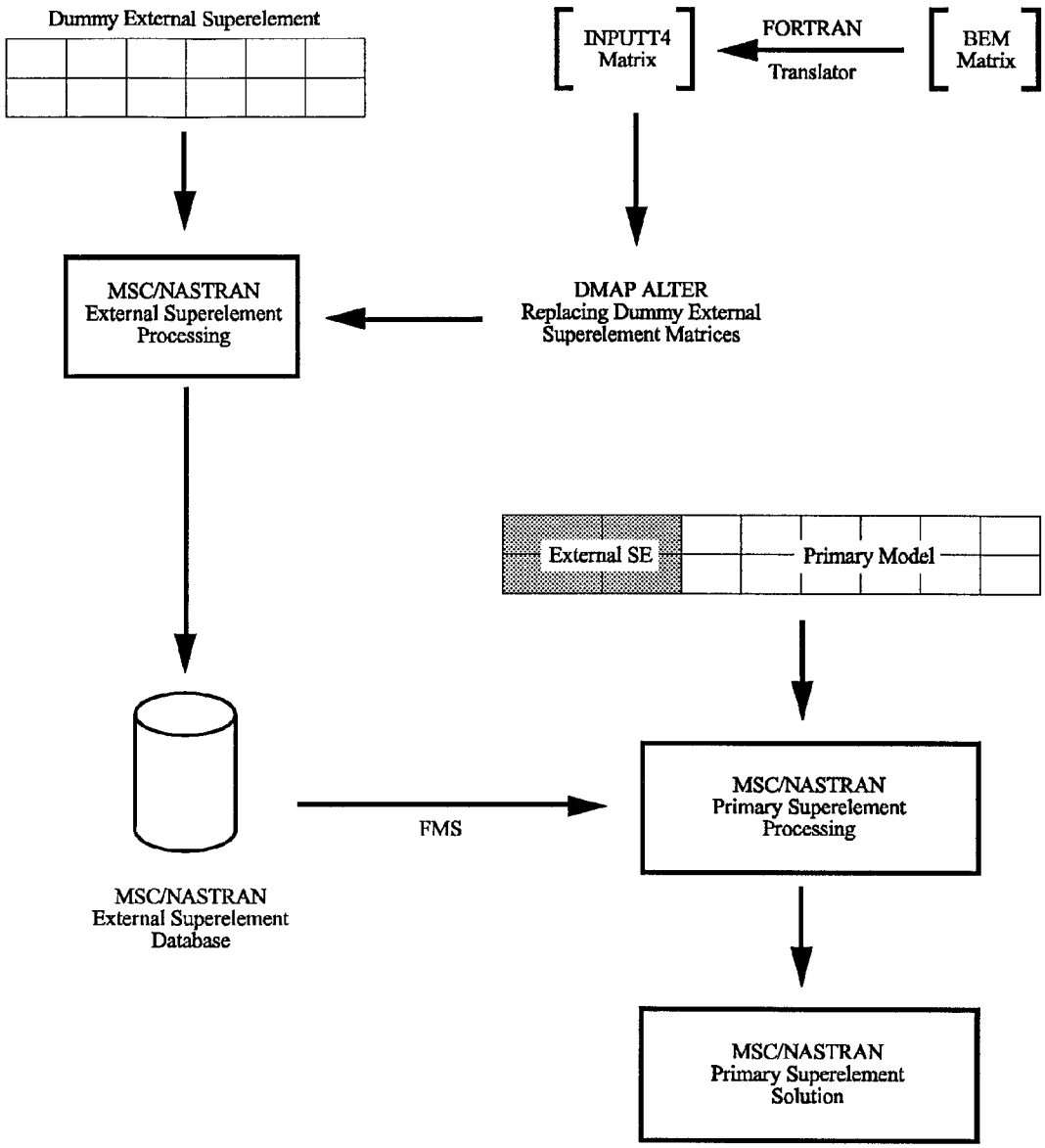

Figure 3. Flow of BEM Matrix Coupling with MSC/NASTRAN

An example of the executive control deck for the external superelement matrix replacement by an BEM matrix is shown in Figure 4. The DMAP alter is simple and can be stored in a library. The DMAP can then be called up with the RFALTER executive control card. The formatted option of the INPUTT4 module was chosen for translation verification checks.

The DMAP alter in Figure 4 could no doubt be reproduced by an independent stand alone DMAP sequence. This is a refinement to the overall method that is planned for the future. The immediate goal was to correctly get the BEM matrix into the MSC/NASTRAN database. The external superelement method supplied the quickest and least error prone path.

```
$
$ ASSIGN FILES FOR THE INPUTT4 ALTERS FOR PA AND KAA
$
ASSIGN INPUTT4='DUB4:[USER.MMCNAMEE.EXTSE]MAP1K.BEM',UNIT=12,
        FORM=FORMATTED
ASSIGN INPUTT4='DUB4:[USER.MMCNAMEE.EXTSE]MAP1P.BEM',UNIT=11,
        FORM=FORMATTED
$
ASSIGN MASTER='DUB4:[USER.MMCNAMEE.EXTSE]MAP1EXT.MASTER'
ASSIGN DBALL='DUB4:[USER.MMCNAMEE.EXTSE]MAP1EXT.DBALL'
ID   IRAD, MAP1
SOL  101
TIME 50
COMPILE DMAP=SELR,SOUIN=MSCSOU,NOLIST,NOREF
ALTER 74,74
INPUTT4 /PAI,,,,/1/11/-1/2  $
MESSAGE //'INPUTT4 FOR PA - BEM COMPLETE' $
ADD PAI,/PA $
ENDALTER
COMPILE DMAP=SEKR,SOUIN=MSCSOU,NOLIST,NOREF
ALTER 124,124
INPUTT4 /KAAI,,,,/1/12/-1/2  $
MESSAGE //'INPUTT4 FOR KAA - BEM COMPLETE' $
ADD KAAI,/KAA $
ENDALTER
CEND
```

Figure 4. Executive Control Deck for BEM External Superelement

The DMAP sequence in Figure 5 shows how the external BEM superelement is accessed by the primary data deck. Accessing the BEM external superelement is identical to accessing a FEM external superelement. The primary superelement deck does not require any special DMAP alters and the CSUPER card provides the connection data. The CSUPER bulk data card also provides the information for merging the external superelement BEM matrices into the MSC/NASTRAN matrices. Database location uses the standard FMS statements for external superelements.

```
ASSIGN MASTER='DUB4:[USER.MMCNAMEE.EXTSE]MAP1.MASTER'
ASSIGN DBALL='DUB4:[USER.MMCNAMEE.EXTSE]MAP1.DBALL'
$
ASSIGN MAP1EXT='DUB4:[USER.MMCNAMEE.EXTSE]MAP1EXT.MASTER'
$
$  LOCATE THE KAA AND PS DATABLOCKS
$
DBLOCATE DB=(KAA,PA) LOGICAL=MAP1EXT
$ ----------------------------------------------------
ID    IRAD, MAP1
SOL   101
TIME  50
CEND
```

Figure 5. Executive Control Deck for Primary Superelement

Analysis Examples

Example 1

The first test structure is a three inch by three inch square plate shown in Figure 6. The loading and boundary conditions were chosen to provide a simple theoretical solution to compare results. Only the membrane properties of the plate elements were activated on the PSHELL property card. The MSC/NASTRAN QUAD4 and QUAD8 plate elements were used to model the FEM region.

The pressure load was equally distributed to each element. Loading was applied with the FORCE static load card at the gridpoints along line A-B. Load magnitudes were defined according to the point loading of the QUAD4 and QUAD8 elements. The load on the QUAD8 element was distributed as one sixth to the corner grid points and two thirds to the midside grid point. The problem was meshed with five different element maps to study accuracy and convergence. Table 1 defines the element mappings.

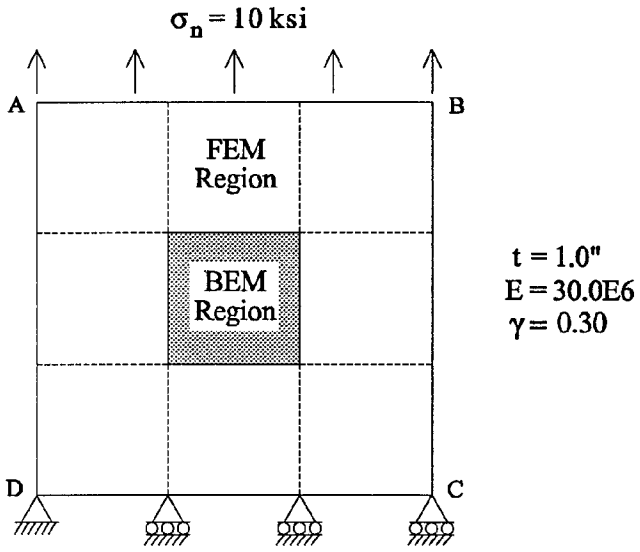

Figure 6. Square Plate Under Tension

Element map 1 breaks the plate into 9 regions as shown by the dotted lines in Figure 6. The center region is modeled by the BEM program for all five element mappings. The second element map breaks up each element from map 1 into four elements. The third element map breaks up each element from map 1 into nine elements. Map 4 replaces the QUAD4 elements in map 1 with QUAD8 elements. Map 5 replaces the QUAD4 elements in map 2 with QUAD8 elements.

Table 1. Example 1 BEM/FEM Mesh Maps

Map	1	2	3	4	5
No. of boundary elements	4 linear	8 linear	16 linear	4 quadratic	8 quadratic
No. of finite elements	8 QUAD4	32 QUAD4	84 QUAD4	8 QUAD8	32 QUAD8
Total grid points	16	48	112	40	128

The results of the MSC/NASTRAN and BEM coupling for all of the mappings is shown in Table 2.

Table 2. Example 1 Numerical Results

	Theory	Map 1	Map 2	Map 3	Map 4	Map 5
Average u_y on Line AB (x 1000 in)	1.000	1.034	1.007	1.003	1.004	1.001
Deviation		(3.36%)	(0.67%)	(0.26%)	(0.40%)	(0.12%)
Average u_x on Line BC (x 1000 in)	-0.300	-0.291	-0.300	-0.301	-0.299	-0.300
Deviation		(3.10%)	(0.03%)	(0.17%)	(0.18%)	(0.12%)
Maximum σ_{xx} psi	0	104	95	30	171	64
Deviation as a % of σ_n		(1.0%)	(1.0%)	(0.3%)	(1.7%)	(0.6%)
Maximum σ_{xy} psi	0	137	100	14	370	57
Deviation as a % of σ_n		(1.4%)	(1.0%)	(0.1%)	(3.7%)	(0.6%)

Discussion

Table 2 shows the general convergence of the displacement and stress results for both the QUAD4 and QUAD8 elements. The results are in good agreement with the theoretical results and are excellent for engineering purposes. The displacements are within one percent error for maps 2, 3 and 5.

Example 2

The second structural example is the simple cantilever beam shown in Figure 7. The beam was divided into two equal sections, one half representing the BEM model and the other half representing the FEM model.

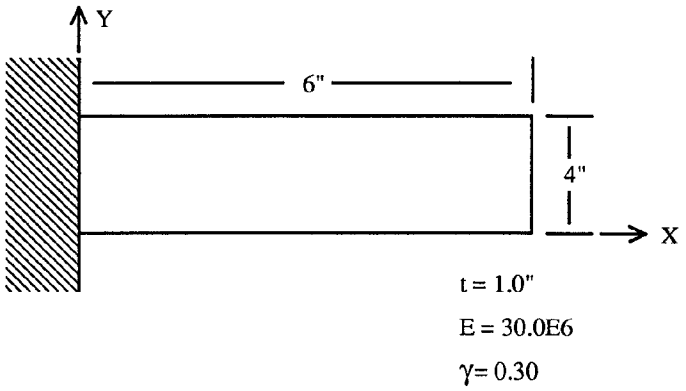

Figure 7. Cantilever Test Structure

The first FEM element mapping divided the FEM section of the cantilever beam into a two by six mesh with QUAD4 elements. As in example 1, only the membrane properties were activated on the PSHELL property card. The overall structural model is shown in Figure 8. Point loads were applied to the grid points 7, 14 and 21 with the FORCE card. The total magnitude of the load was 30 pounds. The FEM model and loads were constructed to provide symmetric results for easy comparison and analysis.

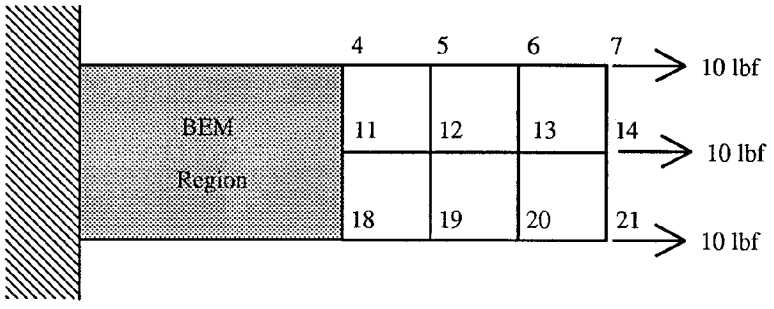

Figure 8. BEM - FEM Breakdown of Cantilever Beam - Example 2

A full FEM analysis was performed on the cantilever beam for a solution comparison. The comparison of the displacements between the FEM model and BEM-FEM model are shown in Table 3.

Table 3. Example 2 Numerical Results

Grid	X - FEM	X - BEM-FEM	Y - FEM	Y - BEM-FEM
4	1.477819E-06	1.502660E-06	-1.662866E-07	-2.074882E-08
5	1.969526E-06	1.990541E-06	-1.663618E-07	-1.768832E-07
6	2.483508E-06	2.486602E-06	-9.458405E-08	-9.827090E-08
7	3.251300E-06	3.254904E-06	-2.996288E-07	-2.978411E-07
11	1.478370E-06	1.502713E-06	-4.671089E-21	-7.411865E-13
12	1.987537E-06	1.971150E-06	-7.505837E-21	-6.498282E-14
13	2.450768E-06	2.456990E-06	-1.055482E-20	5.952593E-13
14	2.704165E-06	2.710506E-06	-1.363194E-20	1.259689E-12
18	1.477819E-06	1.502661E-06	1.662866E-07	2.074739E-08
19	1.969526E-06	1.990543E-06	1.663618E-07	1.768830E-07
20	2.483508E-06	2.486603E-06	9.458405E-08	9.827209E-08
21	3.251300E-06	3.254906E-06	2.996288E-07	2.978436E-07

The displacements of grid points 4 through 7 have been plotted in Figure 9 for a visual comparison.

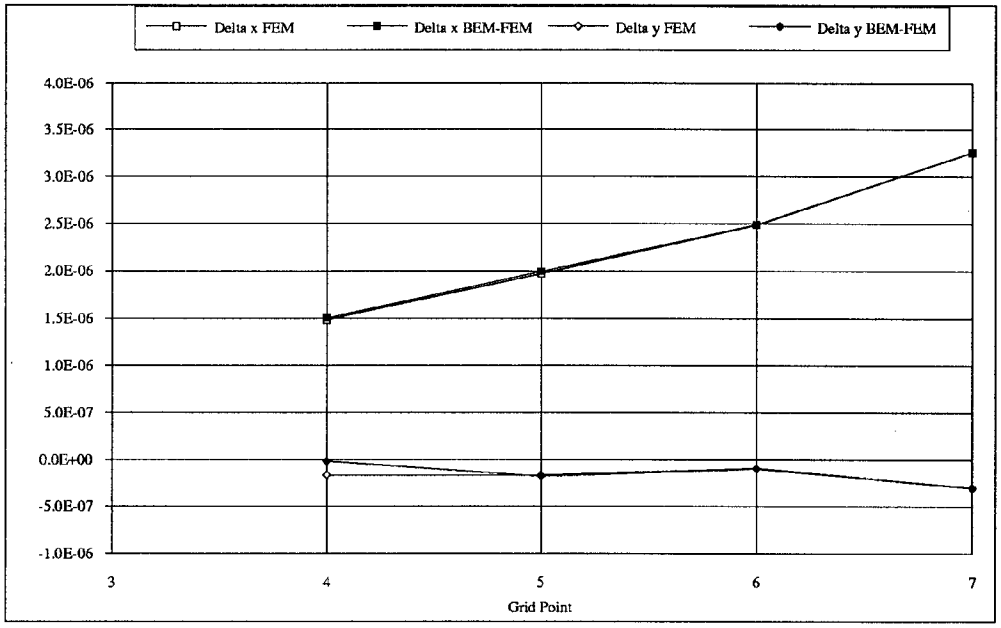

Figure 9. Example 2 Displacements of Grid Points 4 through 7

Discussion

Figure 9 shows that the Δx displacements are very close except at the interface. Percentages calculated from the Table 3 results show the BEM-FEM interface Δx displacements are nearly two percent higher than the FEM Δx displacements. All other BEM-FEM gridpoints show a Δx displacement that is less than 1 percent higher that the comparable FEM model grid point Δx displacement. Further analysis on the Δy displacements show that the BEM-FEM model is 87 percent lower than the FEM interface grid point Δy displacements.

Example 3

The cantilever beam from example 2 was modified by doubling the mesh density and applying a uniform load over the tip. The element type was changed to QUAD8. The selection of mesh refinement and change in element type was done to help in understanding the results of example 2. Figure 10 shows the modifications. The mesh density and QUAD8 elements not allow showing the ID of every grid point. The displacements of gridpoints along lines A-B, C-D and E-F will be examined. The load was applied with the FORCE card and in a manner to produce symmetric results. A FEM model of the complete cantilever was built to provide results comparisons.

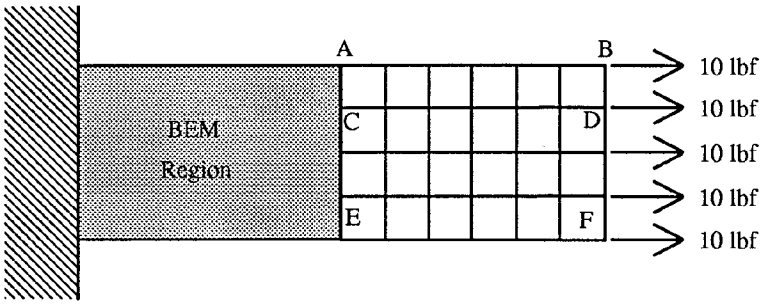

Figure 10. BEM - FEM Breakdown of Cantilever Beam - Example 3

The displacements for the grid points in the FEM portion of the model are shown in Table 4.

Table 4. Example 3 Numerical Results

Grid	X - FEM	X - BEM-FEM	Y - FEM	Y - BEM-FEM
A-B				
13	2.472240E-06	2.484436E-06	-2.752352E-07	-2.830153E-07
14	2.679640E-06	2.690251E-06	-2.744380E-07	-2.768905E-07
15	2.886987E-06	2.897069E-06	-2.727328E-07	-2.744441E-07
16	3.095286E-06	3.104097E-06	-2.700702E-07	-2.715578E-07
17	3.304440E-06	3.312713E-06	-2.668120E-07	-2.680217E-07
18	3.509166E-06	3.517486E-06	-2.601577E-07	-2.608940E-07
19	3.718900E-06	3.727313E-06	-2.449351E-07	-2.454692E-07
20	3.957447E-06	3.965835E-06	-2.298214E-07	-2.303025E-07
21	4.212234E-06	4.220628E-06	-2.355563E-07	-2.359951E-07
22	4.401194E-06	4.409618E-06	-2.382209E-07	-2.386268E-07
23	4.643892E-06	4.652337E-06	-1.845369E-07	-1.849351E-07
24	5.425902E-06	5.434348E-06	-2.308014E-07	-2.312025E-07
25	6.331167E-06	6.339611E-06	-1.200725E-06	-1.201123E-06
C-D				
51	2.473594E-06	2.476178E-06	-1.377886E-07	-1.375122E-07
52	2.681839E-06	2.688064E-06	-1.371057E-07	-1.392621E-07
53	2.890077E-06	2.898272E-06	-1.358150E-07	-1.371670E-07
54	3.099045E-06	3.107535E-06	-1.337962E-07	-1.350765E-07
55	3.307970E-06	3.316324E-06	-1.297452E-07	-1.307750E-07
56	3.512833E-06	3.521241E-06	-1.223815E-07	-1.231123E-07
57	3.716237E-06	3.724712E-06	-1.116837E-07	-1.122115E-07
58	3.932514E-06	3.940988E-06	-1.007109E-07	-1.011602E-07
59	4.147128E-06	4.155590E-06	-8.614607E-08	-8.656711E-08
60	4.294597E-06	4.303057E-06	-6.204230E-08	-6.244453E-08
61	4.412451E-06	4.420913E-06	-6.619814E-08	-6.659686E-08
62	4.743469E-06	4.751928E-06	-2.188838E-07	-2.192867E-07
63	5.083336E-06	5.091793E-06	-2.895951E-07	-2.899986E-07
E-F				
146	2.472778E-06	2.483859E-06	2.065649E-07	2.087744E-07
147	2.889260E-06	2.898111E-06	2.043226E-07	2.060365E-07
148	3.305363E-06	3.313928E-06	1.976786E-07	1.980369E-07
149	3.732178E-06	3.740531E-06	1.765565E-07	1.764303E-07
150	4.154204E-06	4.162574E-06	1.530607E-07	1.527240E-07
151	4.717441E-06	4.725815E-06	1.067868E-07	1.063818E-07
152	4.880697E-06	4.889075E-06	6.993844E-07	6.989284E-07

The plot in Figure 11 shows the Δx displacements of the gridpoints along Line A-B of Figure 10.

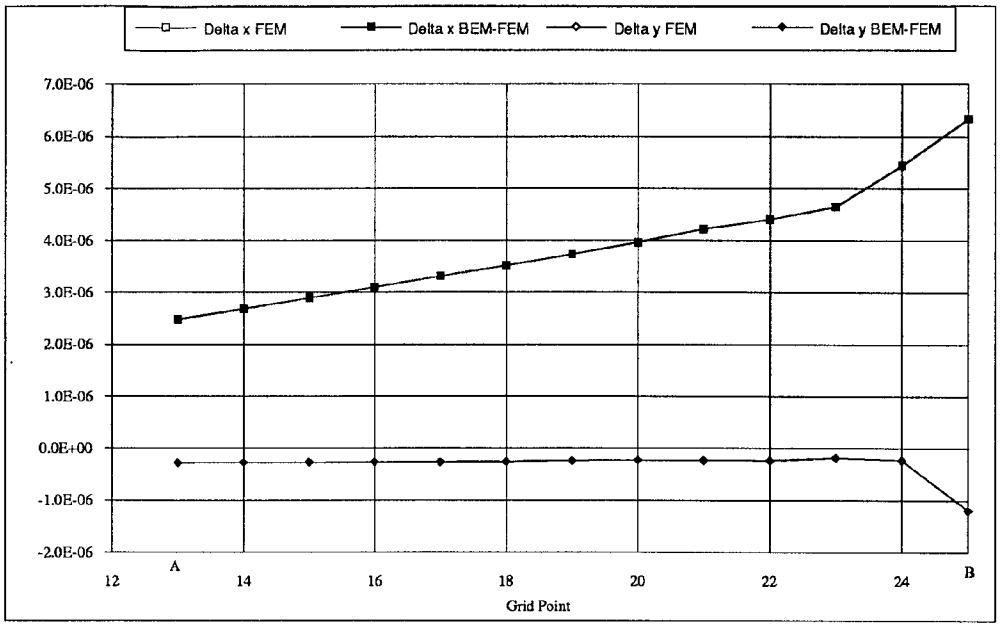

Figure 11. Example 3 Displacements of Grid Points 13 through 25 (Line A-B)

Discussion

Figure 11 shows that the Δx displacements are very close EVEN at the interface. Percentages calculated from the Table 4 results show the BEM-FEM interface Δx displacements are no more that one half of a percent higher than the FEM Δx displacements. Further analysis on the Δy displacements show that the BEM-FEM model is roughly two percent greater than the FEM grid point Δy displacements. The results are within reason and acceptable for engineering purposes.

Conclusions

The mechanics of coupling a BEM matrix to MSC/NASTRAN proved to be exceptionally easy. This is primarily due to the flexibility of superelement programming in the solution sequences. The example problems show that as with FEM models, mesh density and element selection play a role in accuracy of results. The results reinforce the idea of pilot models before full scale usage of any new technique. Overall the results were satisfactory once a reasonable mesh/element combination was achieved. The example problems have demonstrated the feasibility and the advantages of coupling the BEM and FEM methods.

References

1. Zienkiewicz, O. C., Kelly, D. W. and Bettess, P., "The coupling of the finite element method and boundary solution procedures", *Int. J. for Num. Meth. in Engng.*, Vol. 11, 1977, pp. 355-375.
2. Brebbia, C. A. and Georgiou, P., "Combination of boundary and finite elements for elastostatics", *Appl. Math. Modelling*, Vol. 3, 1979, pp. 212-220.
3. Kohno, K., Tsunada, T., Seto, H. and Tanaka, M., "Hybrid stress analysis of boundary and finite elements by super-element method", in *Advances in Boundary Elements, Vol. 3: Stress Analysis*, (Eds. Brebbia, C. A. and Connor, J. J.), Springer-Verlag, Berlin, 1989, pp. 27-38.
4. Tullberg, O. and Bolteus, L., "A critical study of different boundary element stiffness matrices", in *Boundary Element Methods in Engineering*, (Ed. Brebbia, C. A.), Springer-Verlag, Berlin, 1982, pp. 621-635.
5. Mang, H. A., Torzicky, P. and Chen, Z. Y., "On the mechanical inconsistency of symmetrization of unsymmetric coupling matrices for BEFEM discretizations of solids", *Computational Mechanics*, Vol. 4, 1989, pp. 301-308.
6. DeFigueiredo, T. G. B., *A New Boundary Element Formulation in Engineering*, Springer-Verlag, Berlin, 1991.
7. Leung, K. L., Chyou, H. H. and Zavareh, P. B., "A Mixed-Hybrid Variational Formulation for Coupling BEM and FEM in Elastostatics", in *Boundary Element Methods–Fundamentals and Applications*, (Eds. Kobayashi, S. and Nishimura, N.), Springer-Verlag, Berlin, 1991, pp. 222-231.
8. Leung, K. L., Zavareh, P. B. and Beskos, D.E., "Coupling of Symmetric BEM and FEM in Elastostatics", Proceedings of the International Conference on Computational Engineering Science, Hong Kong, 1992.
9. *MSC-NASTRAN User's Manual*, Version 67, The MacNeal-Schwendler Corporation, Los Angeles, CA, August 1991.
10. *MSC-NASTRAN Handbook for Superelement Analysis*, Version 61, The MacNeal-Schwendler Corporation, Los Angeles, CA, April 1982.
11. Timoshenko, S.P. and Goodier, J.N., *Theory of Elasticity*, 3rd Edition, McGraw Hill, New York, 1970.